Dear Author,

Please, note that changes made to the HTML content will be added to the article before publication, but are not reflected in this PDF.

Note also that this file should not be used for submitting corrections.

RSC Advances c6ra03864f

PAPER

1

A bactericidal microfluidic device constructed using nano-textured black silicon

Xue Wen Wang, Chris M. Bhadra, Thi Hoang Yen Dang, Ričardas Buividas, James Wang, Russell J. Crawford, Elena P. Ivanova and Saulius Juodkazis

Nano-structured black silicon (bSi) was used as a substratum for the construction of a microfluidic device to test the bactericidal action of this nano-textured surface against *Pseudomonas aeruginosa* bacteria.

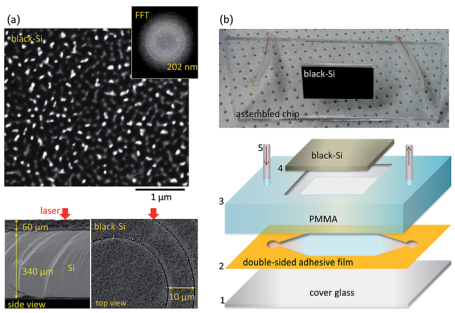

Please check this proof carefully. **Our staff will not read it in detail after you have submitted your proof corrections.**

Translation errors between word-processor files and typesetting systems can occur so the whole proof needs to be read. Please pay particular attention to: tabulated material; equations; numerical data; figures and graphics; and references. If you have not already indicated the corresponding author(s) please mark their name(s) with an asterisk. Corrections at this stage should be minor and not involve extensive changes. Please do not directly edit the text within the PDF file or send a revised manuscript. All corrections must be submitted at the same time.

Please bear in mind that minor layout improvements, e.g. in line breaking, table widths and graphic placement, are routinely applied to the final version.

We will publish articles on the web as soon as possible after receiving your corrections; **no late corrections will be made.**

Please return your **final** corrections, where possible within **48 hours** of receipt following the instructions in the proof notification email.

Queries for the attention of the authors

Journal: **RSC Advances**

Paper: **c6ra03864f**

Title: **A bactericidal microfluidic device constructed using nano-textured black silicon**

Editor's queries are marked like this... **1**, and for your convenience line numbers are inserted like this... 5

Please ensure that all queries are answered when returning your proof corrections so that publication of your article is not delayed.

Query Reference	Query	Remarks
1	For your information: You can cite this article before you receive notification of the page numbers by using the following format: (authors), RSC Adv., (year), DOI: 10.1039/c6ra03864f.	
2	Please carefully check the spelling of all author names. This is important for the correct indexing and future citation of your article. No late corrections can be made.	
3	Do you wish to indicate the corresponding author(s)? If so, please specify the corresponding author(s).	
4	Please check that the inserted Graphical Abstract image and text are suitable. Please ensure that the text is no longer than 250 characters (including spaces).	
5	Ref. 10 and 33: Please provide the title/journal title and if a journal article, page or article number(s).	
6	Ref. 18: Please give the name of this journal in full, including any other names by which this journal may be known (e.g. Chin. J. Struct. Chem. is also known as Jiegou Huaxue), so that its CASSI abbreviation can be checked for indexing purposes.	
7	Ref. 21, 29 and 53: Please provide the page (or article) number(s).	
8	Ref. 45: Please provide the journal title.	

RSC Advances

PAPER

A bactericidal microfluidic device constructed using nano-textured black silicon

Cite this: DOI: 10.1039/c6ra03864f

Xue Wen Wang,†[ab] Chris M. Bhadra,†[a] Thi Hoang Yen Dang,[a] Ričardas Buividas,[a] James Wang,[a] Russell J. Crawford,[a] Elena P. Ivanova[a] and Saulius Juodkazis[ab]

Received 11th February 2016
Accepted 24th February 2016

DOI: 10.1039/c6ra03864f

www.rsc.org/advances

Nano-structured black silicon (bSi) was used as a substratum for the construction of a microfluidic device to test the bactericidal action of this nano-textured surface against *Pseudomonas aeruginosa* bacteria. A narrow 15 μm high and 1 cm wide flat flow channel was constructed that allowed the bacteria to come into contact with the bactericidal nano-spikes present on the surface of the bSi. The narrow channel within the device was designed such that a single layer of bacterial cells could reside at any given time above the bSi substratum during flow. The large 1 × 2 cm^2 surface area of the bSi was shown to be efficient in being able to kill the bacterial cells, achieving an approximate 99% killing efficiency. The flow rate required to fill the bSi chamber was found to be 0.1 μL s^{-1}, with a 10 min equilibration time being allowed for the bacterial cells to interact with the bSi surface. Complete rupturing of *E. coli* cells was achieved after 15 cycles, allowing the effective release of cellular proteins from within the bacterial cells (65.2 μg mL^{-1} from 3 × 10^8 cells per mL). The channel was then able to be re-used after washing of the cell with 10 successive cycles of sterile MilliQ water. Larger volumes of bacterial suspensions have the potential to be treated using a similar flow channel configuration if the dimensions of the flow channel are scaled accordingly. This bactericidal microfluidic device provides a novel platform for studies carried out under both static and dynamic (flow) conditions.

Introduction

Antibacterial surfaces[1–3] are becoming imperative in applications designed to curb the negative consequences associated with resistance to antibiotics present in food, water, and soil.[4] Bacterial resistance arising from extensive exposure to antibiotics has the potential to compromise our immune system, particularly with regard to our ability to effectively resist bacterial infections. Many natural and synthetic surfaces achieve their self-cleaning, anti-fouling and/or bactericidal properties through various mechanisms; they can be highly oxidative, becoming bactericidal when activated by UV-light[5] self-cleaning due to their surfaces being rendered hydrophobic *via* modification of their chemical or mechanical properties,[6–8] or anti-fouling due to their surface structures sterically hindering the attachment of pathogens.[4,9] Other applications of micro- and nano-structured surfaces in the biomedical industry include dermal patches, which possess painless needles that allow the controlled release of drugs, and bandages that possess bio-compatible microfibers that trigger increased levels of healing when exposed to ultraviolet UV light.[10] Surfaces that display mechanical means for antifouling and antibacterial properties are a topic of significant research as they provide a substrate from which a fundamental understanding of the mechanism takes place.[11–14] These surfaces have wide applications in the production of sanitary surfaces such as mobile telephones and other household items.[15]

The search for inexpensive methods for the fabrication of large area nano-textured surfaces is currently underway. Silicon is a substratum that has been used extensively in the semiconductor and solar cell industries.[16–20] Being a relatively inexpensive product, silicon represents one of the best substrata for the fabrication of large areas of nano-textured surfaces, where reproducible surfaces are currently able to be prepared over surfaces of several centimetres in diameter. Such substrata can also have electrical and photo-electrochemical device level functionalities incorporated into their surface, which is useful when producing micro-chips.[21] Methods for preparing these nano-textured surfaces using a silicon substratum include plasma etching, where the deposition of electrical contacts is required for the fabrication of wafer sized bSi surfaces.[22–26] The unique nano-topography of bSi forms due to the self-organized hard mask that results from the first few seconds of etching. These are specific to the chemistry and chamber materials being used for the production of the bSi.[27] It is used in high efficiency solar cells, as it represents a low reflectance or

[a]Faculty of Science, Engineering and Technology, Swinburne University of Technology, John St., Hawthorn, Vic. 3122, Australia. E-mail: sjuodkazis@swin.edu.au; eivanova@swin.edu.au; Fax: +61 3 9214 5435; Tel: +61 3 9214 8718

[b]Melbourne Centre for Nanofabrication (MCN), Australian National Fabrication Facility (ANFF), Clayton, VIC 3168, Australia

† X. W. W. and C. M. B. have contributed equally.

This journal is © The Royal Society of Chemistry 2016

broadband absorbing surface. More recently it has been used for the production of sensors that are based on surface enhanced Raman scattering (SERS).[28] bSi substrata have recently been produced that possess a similar surface topography to that of dragonfly wings, and have been found to exhibit a similar bactericidal efficiency when coming in contact with pathogenic bacteria and spores.[29]

Given this demonstrated bactericidal functionality of the bSi surface, a microfluidic device was constructed incorporating a bSi substrate to investigate whether this bactericidal action would be effectively translated within a flow channel of a microfluidic device. Applications of such devices, if effective, would be of great benefit in many different fields, such as in the pharmaceutical industry for the detection and/or monitoring of bacterial contamination.

Experimental

The bSi was prepared using a plasma etching process.[28,30] An Oxford PlasmaLab 100 ICP380 plasma etcher was used for patterning the surface of p-type boron-doped 4-inch diameter silicon wafers of specific resistivity 10–20 Ω cm^{-1}, having a ⟨100⟩ oriented surface (Atecom Ltd, Taiwan). The resulting surface possessed pencil-like nano-spikes that were approximately 500 nm in height and 20 nm in pillar diameter. The lateral distribution was relatively random, with a distance between neighbouring spikes being approximately 45 ± 20 nm. The lateral distribution of the needles was determined from fast Fourier transform (FFT) processing of the SEM images (Fig. 1(a)). The static water contact angle on the bSi was measured to be approximately 101°, displaying a similar hydrophobicity to that previously reported for bSi prepared under the same conditions.[29,31] Unmodified silicon wafers were used as control surfaces.

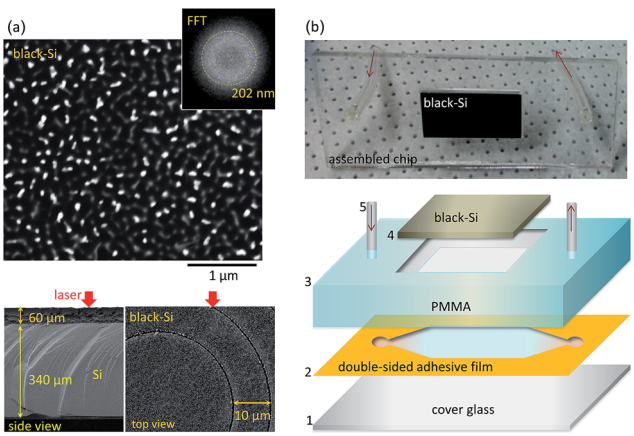

Fig. 1 (a) (top) High resolution SEM image of bSi with a fast Fourier transform (FFT) image (inset). (bottom) Side and top view SEM images of laser scribed line used for cleaving the 400 µm thick Si wafer. (b) (top) Micrograph of the assembled chip and a schematic diagram of the chip assembly (1 to 5), with the adhesive film determining the channel height of ~15 µm. The area of the bSi is 2 × 1 cm^2, and the time required to fill the channel above the bSi at a flow rate of 0.1 µL s^{-1} was 30 s.

The bSi and silicon wafers were precisely cut using a femtosecond laser (Pharos, Light Conversion Ltd.) at a wavelength of $\lambda = 515$ nm, pulse duration of 230 fs, pulse energy 7 µJ per pulse at repetition rate of 100 kHz and scan speed 1 mm s^{-1}. The resulting wafer was mounted on 3-axis stage with 5 nm repetition accuracy (Areotech Ltd.). The beam was focused to a 0.9 µm spot by an objective lens with a numerical aperture NA = 0.7 ($d = 1.22\lambda/\mathrm{NA}$). The line scribing process was repeated 7 times and took 40 min to scribe a single 4-inch wafer into 20 × 10 mm^2 pieces, which would be used for construction of the micro-fluidic chip (Fig. 1). The scribing depth reached approximately 60 µm which was sufficient for clean cleavage of the wafer (Fig. 1). The lateral width of the laser cut was only 2–3 times wider than the focal spot diameter. An arbitrary substratum shape could be prepared using this procedure (see circular cuts in Fig. 1(a)).

The microfluidic chip was assembled *via* a simple method using an adhesive tape spacer, which allowed the shape and height of the microfluidic channel to be defined.[30,32] In such a design, an adhesive double sided tape (ARclad IS-8026-15, Adhesives Research Inc.) was placed on the glass substratum with the channel layout being defined by a laser cutter (CO_2 laser VLS 2.30, Versa Laser). The chip was completed by placing the top plate of the bSi in position and sealing the device with silicone. The tubing, obtained from syringe needles, was added and sealed in position, as required. Duplicate chips, fabricated using the control silicon wafer substrates, were used as negative controls. The channel height of both the bSi and control chips was 15 µm, determined by the thickness of the adhesive tape used in the construction of the device. This height was selected in order to accommodate the rod-shaped *P. aeruginosa* cells, which had dimensions of approximately 2 µm × 1 µm.[33]

P. aeruginosa ATCC 9027 and *E. coli* K 12 cells, obtained from the American Type Culture Collection (ATCC, USA), were used this study. Bacterial stocks were prepared in 20% glycerol nutrient broth (Oxoid) and stored at −80 °C until needed. Prior to each experiment, the bacterial cultures were refreshed from the stock solution on nutrient agar (Oxoid), and a fresh bacterial suspension was prepared from bacterial cells, which were grown overnight in 100 mL of nutrient broth (in 0.5 L Erlenmeyer flasks at 37 °C with shaking at 120 rpm). Bacterial cells were collected at the logarithmic stage of growth (data not shown). The *P. aeruginosa* bacterial suspension was adjusted to $OD_{600} = 0.1$ and diluted to produce bacterial suspension with an infectious dose of 10^5 cells per mL in a 10 mM phosphate buffer solution (PBS), pH 7.4. A peristaltic pump (Minipuls evolution, Gilson Inc.) was used to introduce an infectious dose of *P. aeruginosa* cells into the micro-fluidic chip at a flow speed of 0.1 µL s^{-1}. A 3.2 µL aliquot was taken from the output and incubated on agar plates for 12 hours at 37 °C (Memmert, Heraeus CO_2 incubator) to allow the colony forming units to be determined. All experiments were performed at room temperature (*ca.* 25 °C), with at least three independent experiments being performed. Viability assays were performed using standard plate counts,[34] where colonies were counted and the number of colony forming units (cfu) per millilitre was calculated. The calculated cfu numbers were assumed to be

 This journal is © The Royal Society of Chemistry 2016

equivalent to the number of live cells present in suspension.[34] The bactericidal efficiency was measured as the number of inactivated cells per cm^2 of sample per minute, relative to the control surfaces. All experiments were completed within 3 h.

The bacterial solution was passed through the channel with a 10 min pause between repeated passes through the device (Fig. 2). Each experiment was repeated three times. The filling time required for the entire volume of the channel was found to be 45 s. Repeated cycles were timed in such a way that an equivalent volume of solution was used to fill the cell using a forward and reverse rotation of the pump.

The bactericidal effect of the microfluidic bSi channel was also evaluated after each cycle by staining the dead and live cells, which were then visualised. Non-viable bacterial cells are stained red with propidium iodide, whereas the living bacteria are stained green with SYTO 9 (Molecular Probes, Invitrogen, Grand Island, NY, USA). Imaging was carried out using a Fluorview FV10i Confocal System with a water immersion objective lens (UPLSAPO 60W) with a NA of 1.2 and working distance of 2 mm. This allowed a large field of view at a very high resolution $0.61\lambda/NA \approx 0.5$ μm for the optimised red-green spectral range of imaging; here λ is the wavelength of fluorescence. In addition, the cells of the surface of the flow channel were visualised using scanning electron microscopy (SEM). SEM images were obtained using a field-emission FESEM (ZEISS SUPRA 40VP) tool at 3 kV under magnification values of 1 k×, 5 k× and 20 k× respectively, as previously described.[29]

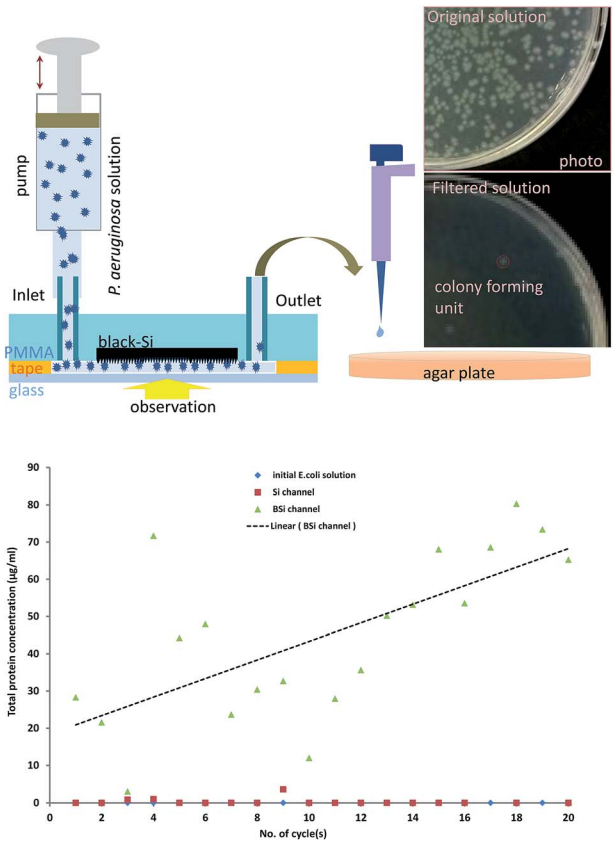

Fig. 2 Schematic diagram of the bacterial solution filtration process through the bSi-containing microfluidic chip, with the subsequent viability tests. An optical image, showing the recovered *P. aeruginosa* cells before and after treatment with the microfluidic cell, is provided.

The flow channel was tested to evaluate its efficiency in achieving total cellular protein release from the ruptured *E. coli* K 12 cells (Fig. 2). Before each experiment, the bacterial suspension was adjusted to $OD_{600} = 0.1$. A peristaltic pump (Minipuls evolution, Gilson Inc.) was used to introduce the *E. coli* suspension (cell density of 3×10^8 cells per mL) into the micro-fluidic chip. The bacterial cell suspension was subjected to 20 repeated cycles through the microfluidic device at a flow speed of 0.1 mL s^{-1}. A 50 μL portion (in triplicate) of the suspension was collected after each cycle and the resulting total protein concentration was quantified using a Bradford protein assay[35–38] using a NanoDrop 2000 (ThermoFisher, Australia). The total concentration of proteins from *E. coli* cells lysed using enzyme treatment and sonication was determined as described elsewhere[39–41] for comparative purposes.

To test whether this microfluidic device was able to be re-used, a washing procedure was adopted whereby the device was initially flushed using PBS buffer solution for 4 s, followed by washing with distilled water at speed of 5.7 μL s^{-1} for up to 20 cycles. A forward and backward flow switching procedure was carried out using the peristaltic pump for 2 s intervals in each flow direction, with a total washing time of 4 s being used. Several microfluidic channels were fabricated to allow a comparison of the consistency between tests.

Results

The flow cell dimensions were optimised to achieve efficient elimination of bacterial cells by restricting the instances of several bacterial cells being present within the cells on top of each other, maximising their exposure to the nano-textured surface of the black silicon. The fabricated microfluidic device contained a 2×1 cm^2 section of bSi, with a 15 μm gap above the bactericidal surface of the bSi, which is almost a twofold reduction in available volume compared with previous cell designs.[42] This reduction in volume was essential in order to ensure an efficient interaction occurred between the bSi surface and the bacterial suspension during flow. The wall effect causes a larger viscous drag near the substrate[43] with a faster flow being present in the centre of the cell. This means that there was a greater probability that bacteria could be located at the centre, or mid-height, of the channel. When the flow was paused for the bacteria to come into contact with the bSi surface, the larger width and large surface area of bSi were also key features of the microfluidic chip. The peristaltic pump was pushing the *P. aeruginosa* cells through the channel, and a uniform advancing front of air–liquid interface was observed under the microscope, confirming the uniform height of the channel over the entire area of the bSi.

The efficient bactericidal action of the bSi surface was confirmed using standard staining techniques using propidium iodide (red) for non-viable and SYTO 9 (green) for viable bacterial cells, respectively (Fig. 3). The SEM images of the bacterial cells on the bSi surface revealed changed cell

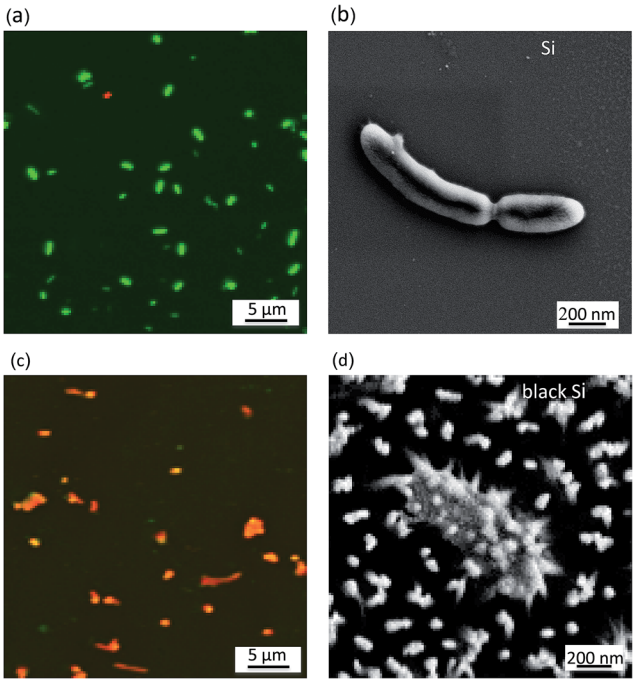

Fig. 3 Bactericidal effect of the flow channel. (a) Micrograph of fluorescently labelled *P. aeruginosa* cells and (b) SEM image of *P. aeruginosa* cells on the silicon control surface. (c) Microscopic and (d) SEM images of *P. aeruginosa* cells on the bSi surface. Confocal images have been taken after 10 min of cell contact with respective substratum. Bacterial cells have been stained with SYTO 9 (green) and propidium iodide (red) indicating live and dead bacteria, respectively.

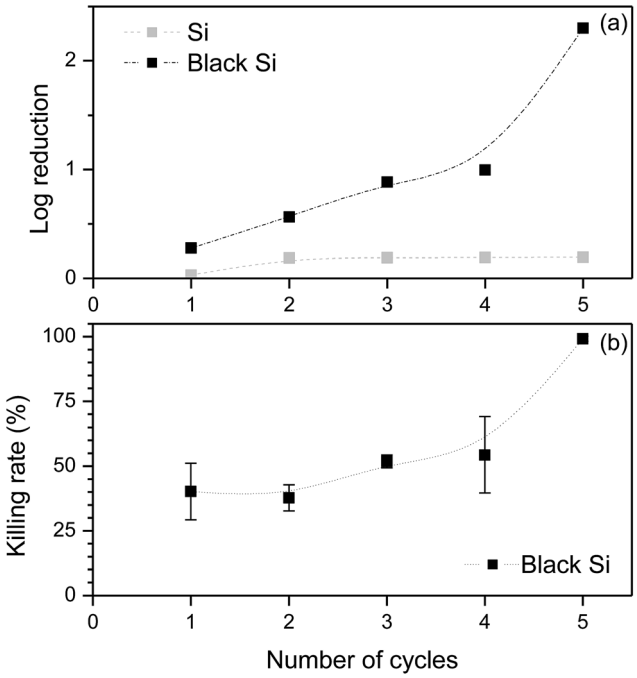

Fig. 4 Bactericidal performance of the bSi-containing microfluidic cell. (a) $\log_{10}$ reduction in the number of *P. aeruginosa* cells as a function of consecutive cycle runs through the device. One cycle corresponds to 45 s of filling the chamber followed by a 10 min stoppage time. (b) The killing rate of bacteria as a function of the number of cycles through the bSi-containing device.

morphology confirming that structural damage to the cells had occurred.

To quantify the bactericidal performance of the flow channel, a portion of bacterial solution that had passed through the microfluidic device was sampled after each cycle and plated onto agar plates. The results presented in Fig. 4(a) demonstrate that the elimination of bacterial cells from the initial suspension was dependent on the number of filtering cycles to which the initial suspension was subjected. A slight reduction in the concentration of bacterial cells was also observed for the control surface, this being likely due to adhesion of the bacterial cells onto the flow channel walls. There was, however, no evidence of damaged bacterial cells present on the microfluidic channel with the control silicon surface, as confirmed by confocal and SEM image analysis (Fig. 3).

The bactericidal efficiency of the bSi-containing microfluidic device was calculated by subtracting the extent of bacterial removal using the control microfluidic device under the same experimental conditions, the results of which are presented in Fig. 4(b). The bacterial killing rate was calculated as a $\log_{10}$ reduction value to analyse the bactericidal rate on a comparative scale, which revealed that up to 99% of the cells were killed after 5 consecutive cycles through the bSi-containing microfluidic device.

It is crucial to integrate cell lysis and fractionation steps to achieve a total micro analytical system for the analysis of cells and their constituent proteins on-chip, without adding extra steps.[44] To determine the same functionality, the microfluidic channel was used to quantify the release of the total cellular proteins from ruptured *E. coli* cells from the cell suspension, which was being circulated through the channel (Fig. 5). The protein concentration was monitored after each cycle and over the entire 15 cycles. An additional 5 cycles were performed to ensure the complete extraction of proteins. Approximately 65.2 µg mL^{-1} of cellular protein was extracted after 15 cycles, as confirmed using Bradford's assay (Table 1). These results are in

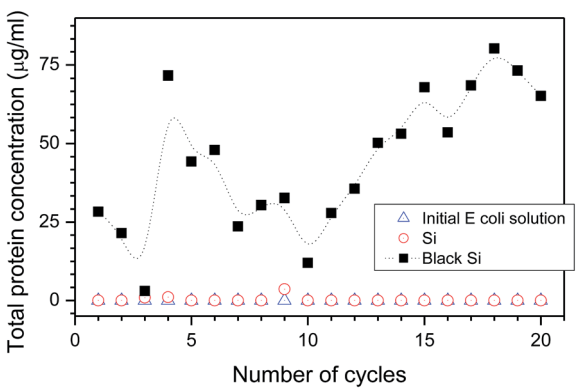

Fig. 5 Estimation of total protein released from ruptured *E. coli* cells. A linear gradient has been drawn to signify the increase in extracted proteins as a function of cycles through the bSi-containing device. The protein extracted from *E. coli* suspensions and the Si-control device has been included for comparison.

 This journal is © The Royal Society of Chemistry 2016

Table 1 Comparative protein extraction from *E. coli* cells

Lysis technique	Protein concentration[a] ($\mu g\ mL^{-1}$)
Theoretical estimation	~60–66
Microfluidic channel	65.2
Sonication	29.6
Enzyme treatment and sonication	52.7

[a] From 3×10^8 cells per mL.

agreement with an estimated amount of 60–66 $\mu g\ mL^{-1}$ of total cellular proteins, which can be obtained from 3×10^8 cells per mL, taking into account that a single *E. coli* cell contains 0.2 pg protein.[45] Notably, it appeared that the combined enzyme and sonication treatment was less efficient at extracting the cellular proteins than the mechanical rupture method that occurred within the microfluidic device, which resulted in a total cellular protein yield of 52.7 $\mu g\ mL^{-1}$.

To assess whether the bSi-containing microfluidic device was able to be cleaned and re-used, a single flush of the device using PBS buffer solution was carried out at a 5.7 $\mu L\ s^{-1}$ flow rate for 4 s followed by 10 successive cycles of MilliQ water. Each flush was carried out at a rate of 5.7 $\mu L\ s^{-1}$ for a period of 4 s, followed by a forward and backward flow for 2 s each. After the washing cycle, there was no evidence of any viable bacteria being present within the device, as confirmed by the direct colony counting technique. The total time required for cleaning the microfluidic device was 1 minute.

Discussion

The 10 minute flow stoppage that occurred during the bacterial flow through the microfluidic device was undertaken to allow the bacterial cells sufficient time to come into contact with the bSi surface within the cell. The average thermal velocity that occurs through this process was estimated by assuming equality between the kinetic and thermal energies taking place. This was calculated using $v = \sqrt{3k_bT/m} \approx 1.0\ mm\ s^{-1}$, where k_b is the Boltzmann constant, $T = 293$ K is the absolute temperature at normal conditions, and m ~10.0 pg is the mass of a single *P. aeruginosa* cell. The mean displacement of bacteria over time (t) occurs due to Brownian motion, and is calculated according to $\Delta x\ (t) = \sqrt{32mtv^2/81\pi\mu r}$ is, where $\mu = 8.9 \times 10^{-4}$ Pa s is the dynamic viscosity of water. It takes only $t \sim 2$ min for bacteria to move over $\Delta x(t) = 15\ \mu m$ which is comparable with the height of the microfluidic channel. During the total exposure period, it is therefore almost certain that the bacteria would have come into contact with the bSi surface within the microfluidic device.

Further studies are now required to systematically investigate the bactericidal action of the bSi-containing microfluidic device against other bacterial types, and to determine the maximum flow rate that can be used that will still achieve an efficient level of bactericidal action.

In our previous study,[42] where a very high flow speed of more than 1 m s^{-1} were used when pumping polystyrene bead suspensions through a microfluidic device with channels containing sharp micron-sized features, the beads were seen to be able to avoid contact with the sharp features by following the laminar flow within the channel. Since the bSi components of the microfluidic devices used in the current study were prepared from 4-inch wafers, it is possible to construct a microfluidic device that contains wider and longer bSi sections, and perhaps to also contain multiple bSi channels for sequentially treating bacterial solutions. Studies involving such components would reveal whether it is possible to design a device for testing the bacterial contamination of grey water. The bactericidal action of the bSi component of the microfluidic devices could be further improved by incorporating ultraviolet light-emitting diodes, making such devices applicable to a wide range of water disinfection and sterilisation applications.[46–50] The microfluidic device reported here has demonstrated that it has a high sensitivity for the refractive index of the solution being used; $\Delta\lambda/\Delta n = 390$ nm per RIU (refractive index units)[20] and could be further assessed for its ability to recognise bacterial (or other) contamination by incorporating a section within the device that contains Fabry–Pérot mirrors on the upper and lower walls of the channel. Such a microfluidic device would allow the *in situ* monitoring of refractive index changes that could be related to the removal of bacteria from solution.

An additive pressure (ΔP), scales linearly with the flow velocity (v) in the microfluidic device, for a liquid of viscosity (μ), inside a channel with the transverse dimension height (t), width (w) and length (l) according to: $\Delta P \propto \mu v l/(tw)$.[51] Hence for a longer and narrower channel, ΔP would increase with the second power of the decreasing geometrical length and height dimensions. To maintain a high throughput flow at as large as practical, the width of the channel should be increased.

Micro and nano-fabricated devices have been designed to expedite applied and basic research into cell biology and morphology in dynamic flow through these devices.[52–55] Protein analysis and quantification in clinical samples, such as blood serum or whole-cell lysates presents certain challenges[56] such as in the pre-treatment or fractionation of complex samples for integration into the micro-analysis systems. Several groups have developed microchip- or capillary-based two-dimensional separation systems, which are an integration of micellar electrokinetic chromatography (MEKC) or isoelectric focusing (IEF) with capillary electrophoresis.[57–61] These reports are, however limited by the fact that they are quite complex systems, and a number of additional steps become involved in the separation and identification of the desired protein analyte. A study has also been published where *E. coli* cells have been lysed using a simple channel mechanism.[62] This study, however, uses detergent addition as an additional step to lyse the cells in flow, with the height and depth of the cell being 1000 μm and 100 μm, respectively. Such width and height could be detrimental to the attachment pattern of bacteria, which are not more than 5 μm in their average dimension. Another study incorporated a surface chemistry technique to detect *E. coli* cells in clinical samples. *E. coli* cells have been made to interact with specific antibodies for detection.[63] The device reported in this current study avoids these extra steps, as the bactericidal bSi

surfaces have already been incorporated inside the channel to lyse the cells. Moreover, the height of the channel is such that it ensures the bacteria coming into a contact with the bSi. Moreover, the width of channel can be controlled by mechanically applied pressure.

Conclusions

In this study, a simple method was used to fabricate a microfluidic device containing a channel that was 15 μm in height over a relatively large 2 cm^2 area. Incorporation of bSi into the device design resulted in a device that was bactericidal when flow into the cell was paused for 10 min after filling the cell, which took 45 s. Approximately 99% of *P. aeruginosa* cells from the infectious dose were eliminated after 5 successive fill-stop cycles through the device. The bacterial killing rate was found to be 2.3×10^3 cfu min^{-1} cm^{-2}. The newly designed microfluidic device was also used for the effective extraction of cellular protein from the ruptured *E. coli* bacterial cells. The device was shown to be able to be re-used after washing using a simple high speed flushing process.

The proposed simple microfluidic device containing the nanotextured bSi could be used for surface enhanced Raman spectroscopy applications under the required flow conditions. The device also has the capacity of incorporating electrodes to carry out electrochemical surface cleaning (oxidation of adventitious carbon) or/and removal of oxide.[52] Such flow devices that have the potential for controlling the electrochemical potential are expected to be useful for investigations into detailed surface chemical reactions and catalysis, *e.g.*, in the generation of hydrogen.[64,65] The evolution of oxygen through such electrodes could be achieved if an oxidative stress could be applied to the bacterial cells. The incorporation of UV-LED treatment sections into the device would also be possible.

Acknowledgements

Partial support was obtained for this research through an Australian Research Council DP130101205 grant. In addition, the collaborative research project being undertaken with Altechna Ltd., of which this work is a part, is acknowledged. The technical assistance of Dr SHT Nguyen is gratefully acknowledged. X.W.W. and C.M.B. are recipients of Swinburne University Postgraduate Awards. SJ acknowledges the start-up funding of the Nanotechnology facility, available through a strategic infrastructure grant provided from Swinburne University of Technology.

References

1 W. Zhuang, D. Yuan, J. R. Li, Z. Luo, H. C. Zhou, S. Bashir and J. Liu, *Adv. Healthcare Mater.*, 2012, **1**, 225–238.
2 E. P. Ivanova, J. Hasan, H. K. Webb, V. K. Truong, G. S. Watson, J. A. Watson, V. A. Baulin, S. Pogodin, J. Y. Wang and M. J. Tobin, *Small*, 2012, **8**, 2489–2494.
3 A. H. Broderick, A. S. Breitbach, R. Frei, H. E. Blackwell and D. M. Lynn, *Adv. Healthcare Mater.*, 2013, **2**, 993–1000.
4 A. Jain, L. S. Duvvuri, S. Farah, N. Beyth, A. J. Domb and W. Khan, *Adv. Healthcare Mater.*, 2014, **3**, 1969–1985.
5 M. Sakai, M. Nishimura, Y. Morii, T. Furuta, T. Isobe, A. Fujishima and A. Nakajima, *Journal of Materials Science*, 2012, **47**, 8167–8173.
6 T. S. Santra and F. G. Tseng, *Micromachines*, 2013, **4**, 333–356.
7 Y. Kikuchi, K. Sunada, T. Iyoda, K. Hashimoto and A. Fujishima, *J. Photochem. Photobiol., A*, 1997, **106**, 51–56.
8 K. Kairyte, A. Kadys and Z. Luksiene, *J. Photochem. Photobiol., B*, 2013, **128**, 78–84.
9 M. V. Graham and N. C. Cady, *Coatings*, 2014, **4**, 37–59.
10 C. Guimarães, J. An, M. Humar, W. Goth and A. Yun, 2015. 5
11 J. Hasan, R. J. Crawford and E. P. Ivanova, *Trends Biotechnol.*, 2013, **31**, 295–304.
12 H. K. Webb, R. J. Crawford and E. P. Ivanova, in *Antibacterial Surfaces*, Springer, 2015, pp. 1–8.
13 G. D. Bixler and B. Bhushan, *Crit. Rev. Solid State Mater. Sci.*, 2015, **40**, 1–37.
14 M. V. Graham, A. P. Mosier, T. R. Kiehl, A. E. Kaloyeros and N. C. Cady, *Soft Matter*, 2013, **9**, 6235–6244.
15 K.-C. Park, H. J. Choi, C.-H. Chang, R. E. Cohen, G. H. McKinley and G. Barbastathis, *ACS Nano*, 2012, **6**, 3789–3799.
16 A. Mavrokefalos, S. E. Han, S. Yerci, M. S. Branham and G. Chen, *Nano Lett.*, 2012, **12**, 2792–2796.
17 Y. Liu, T. Lai, H. Li, Y. Wang, Z. Mei, H. Liang, Z. Li, F. Zhang, W. Wang and A. Y. Kuznetsov, *Small*, 2012, **8**, 1392–1397.
18 H. Hauser, B. Michl, S. Schwarzkopf, V. Kubler, C. Muller, M. Hermle and B. Blasi, *Photovoltaics, IEEE Journal of*, 2012, **2**, 114–122. 6
19 S. Y. Reece, J. A. Hamel, K. Sung, T. D. Jarvi, A. J. Esswein, J. J. Pijpers and D. G. Nocera, *Science*, 2011, **334**, 645–648.
20 B.-R. Huang, Y.-K. Yang, T.-C. Lin and W.-L. Yang, *Sol. Energy Mater. Sol. Cells*, 2012, **98**, 357–362.
21 H. Savin, P. Repo, G. von Gastrow, P. Ortega, E. Calle, M. Garín and R. Alcubilla, *Nat. Nanotechnol.*, 2015. 7
22 L. Sainiemi, V. Jokinen, A. Shah, M. Shpak, S. Aura, P. Suvanto and S. Franssila, *Adv. Mater.*, 2011, **23**, 122–126.
23 M. Otto, M. Kroll, T. Käsebier, R. Salzer, A. Tünnermann and R. B. Wehrspohn, *Appl. Phys. Lett.*, 2012, **100**, 191603.
24 M. Gaudig, J. Hirsch, T. Schneider, A. N. Sprafke, J. Ziegler, N. Bernhard and R. B. Wehrspohn, *J. Vac. Sci. Technol., A*, 2015, **33**, 05E132.
25 K. Nguyen, D. Abi-Saab, P. Basset, E. Richalot, M. Malak, N. Pavy, F. Flourens, F. Marty, D. Angelescu and Y. Leprince-Wang, *Microsyst. Technol.*, 2012, **18**, 1807–1814.
26 K. Nguyen, P. Basset, F. Marty, Y. Leprince-Wang and T. Bourouina, *J. Appl. Phys.*, 2013, **113**, 194903.
27 H. Jansen, M. De Boer, S. Unnikrishnan, M. Louwerse and M. Elwenspoek, *J. Micromech. Microeng.*, 2009, **19**, 033001.
28 G. Seniutinas, G. Gervinskas, R. Verma, B. D. Gupta, F. Lapierre, P. R. Stoddart, F. Clark, S. L. McArthur and S. Juodkazis, *Opt. Express*, 2015, **23**, 6763–6772.
29 E. P. Ivanova, J. Hasan, H. K. Webb, G. Gervinskas, S. Juodkazis, V. K. Truong, A. H. Wu, R. N. Lamb, V. A. Baulin and G. S. Watson, *Nat. Commun.*, 2013, **4**.

 This journal is © The Royal Society of Chemistry 2016

30 G. Gervinskas, D. Day and S. Juodkazis, *Sens. Actuators, B*, 2011, **159**, 39–43.
31 S. Pogodin, J. Hasan, V. A. Baulin, H. K. Webb, V. K. Truong, T. H. P. Nguyen, V. Boshkovikj, C. J. Fluke, G. S. Watson and J. A. Watson, *Biophys. J.*, 2013, **104**, 835–840.
32 E. P. Ivanova, V. K. Truong, G. Gervinskas, N. Mitik-Dineva, D. Day, R. T. Jones, R. J. Crawford and S. Juodkazis, *Biosens. Bioelectron.*, 2012, **35**, 369–375.
33 I. Vallet-Gely and F. Boccard, 2013.
34 J. Postgate, *Methods Microbiol.*, 1969, **1**, 611–628.
35 H.-K. Ku, H.-M. Lim, K.-H. Oh, H.-J. Yang, J.-S. Jeong and S.-K. Kim, *Anal. Biochem.*, 2013, **434**, 178–180.
36 S. C. Silvério, S. Moreira, A. M. Milagres, E. A. Macedo, J. A. Teixeira and S. I. Mussatto, *Anal. Biochem.*, 2012, **421**, 719–724.
37 N. Carlsson, A. Borde, S. Wölfel, B. Åkerman and A. Larsson, *Anal. Biochem.*, 2011, **411**, 116–121.
38 M. M. Bradford, *Anal. Biochem.*, 1976, **72**, 248–254.
39 P. Shrestha, T. M. Holland and B. C. Bundy, *BioTechniques*, 2012, **53**, 163–174.
40 L. Benov and J. Al-Ibraheem, *J. Biochem. Mol. Biol.*, 2002, **35**, 428–431.
41 R. Mehigh, *Sigma Origins 3*, 2001, pp. 15–16.
42 G. Gervinskas, D. J. Day and S. Juodkazis, *Opt. Mater. Express*, 2012, **2**, 279–286.
43 M. Miwa, S. Juodkazis and H. Misawa, *Jpn. J. Appl. Phys.*, 2000, **39**, 1930.
44 K. Aran, A. Fok, L. A. Sasso, N. Kamdar, Y. Guan, Q. Sun, A. Ündar and J. D. Zahn, *Lab Chip*, 2011, **11**, 2858–2868.
45 G. Carta and A. Jungbauer, Journal, 2010, 364.
46 K. Y. Nelson, D. W. McMartin, C. K. Yost, K. J. Runtz and T. Ono, *Environ. Sci. Pollut. Res.*, 2013, **20**, 5441–5448.
47 M. Shatalov, A. Lunev, X. Hu, O. Bilenko, I. Gaska, W. Sun, J. Yang, A. Dobrinsky, Y. Bilenko and R. Gaska, *Int. J. High Speed Electron. Syst.*, 2012, **21**, 1250011.
48 A. Venancio-Marques, F. Barbaud and D. Baigl, *J. Am. Chem. Soc.*, 2013, **135**, 3218–3223.
49 M. Würtele, T. Kolbe, M. Lipsz, A. Külberg, M. Weyers, M. Kneissl and M. Jekel, *Water Res.*, 2011, **45**, 1481–1489.
50 M. Mori, A. Hamamoto, A. Takahashi, M. Nakano, N. Wakikawa, S. Tachibana, T. Ikehara, Y. Nakaya, M. Akutagawa and Y. Kinouchi, *Med. Biol. Eng. Comput.*, 2007, **45**, 1237–1241.
51 P. Tabeling, *Introduction to microfluidics*, Oxford University Press, 2010.
52 R. Buividas, N. Fahim, J. Juodkazytė and S. Juodkazis, *Appl. Phys. A: Mater. Sci. Process.*, 2014, **114**, 169–175.
53 F. Wu and C. Dekker, *Chem. Soc. Rev.*, 2016.
54 D. Gao, H. Liu, Y. Jiang and J.-M. Lin, *TrAC, Trends Anal. Chem.*, 2012, **35**, 150–164.
55 E. K. Sackmann, A. L. Fulton and D. J. Beebe, *Nature*, 2014, **507**, 181–189.
56 J. El-Ali, P. K. Sorger and K. F. Jensen, *Nature*, 2006, **442**, 403–411.
57 Y.-C. Wang, M. H. Choi and J. Han, *Anal. Chem.*, 2004, **76**, 4426–4431.
58 R. D. Rocklin, R. S. Ramsey and J. M. Ramsey, *Anal. Chem.*, 2000, **72**, 5244–5249.
59 J. Mok, M. N. Mindrinos, R. W. Davis and M. Javanmard, *Proc. Natl. Acad. Sci. U. S. A.*, 2014, **111**, 2110–2115.
60 I. M. Lazar and J. L. Kabulski, *Lab Chip*, 2013, **13**, 2055–2065.
61 R. Hu, X. Feng, P. Chen, M. Fu, H. Chen, L. Guo and B.-F. Liu, *J. Chromatogr. A*, 2011, **1218**, 171–177.
62 E. A. Schilling, A. E. Kamholz and P. Yager, *Anal. Chem.*, 2002, **74**, 1798–1804.
63 S. Wang, F. Inci, T. L. Chaunzwa, A. Ramanujam, A. Vasudevan, S. Subramanian, A. C. F. Ip, B. Sridharan, U. A. Gurkan and U. Demirci, *Int. J. Nanomed.*, 2012, **7**, 2591.
64 J. Juodkazytė, B. Šebeka and S. Juodkazis, *Appl. Surf. Sci.*, 2014, **290**, 13–17.
65 K. Juodkazis, J. Juodkazytė, E. Jelmakas, P. Kalinauskas, I. Valsiūnas, P. Miečinskas and S. Juodkazis, *Opt. Express*, 2010, **18**, A147–A160.

This journal is © The Royal Society of Chemistry 2016